Time Domain Analysis of Propagation Channels in Tunnels

Concepcion Garcia-Pardo, J. Molina-Garcia-Pardo
Information Technologies and Commun. Dept.
Technical Univ. of Cartagena
Cartagena, Spain
[conchi.gpardo; josemaria.molina]@upct.es

Martine Lienard, Pierre Degauque
IEMN/TELICE
University of Lille
Villeneuve d Ascq, France
[martine.lienard; pierre.degauque]@univ-lille1.fr

***Abstract*—Extensive measurement campaigns have been carried out in a road tunnel in a frequency band extending from 2.8 to 5 GHz. From the experimental results, a time domain analysis is performed to study small scale fading, time dispersion of the ultra wide band pulse and correlation between signals received at different locations.**

Keywords- tunnel; impulse response; UWB; delay spread; direction of arrival; correlation.

I. INTRODUCTION

There is now an increased interest for ensuring high bit rate communication and localization in tunnels. As an example, for automatic underground subways, a train to track link allows increasing the performances of maintenance and control-command techniques. Similarly, video surveillance, voice communication and wireless sensor monitoring are of great importance in underground mines. A large number of papers have thus already been published in the literature for studying the narrow band and wide band channel characteristics.

For mine tunnels, the variation of path loss as a function of frequency from 2 GHz to 5 GHz was studied in [1] and a frequency-domain autoregressive model was developed. Various communication links were also considered including both Line-of-Sight (LOS) and non-LOS scenarios [2].

In case of road or railway tunnels, path loss and probability distribution with respect to fading widths deduced from measurements at 2 GHz were detailed in [3], while the effects of pedestrians and vehicles in different road tunnels are studied in [4]. A wideband directional measurement campaign conducted inside an arched highway tunnel is described in [5]. Using a channel sounder centered at 5.2 GHz with a bandwidth of 100 MHz, the spatio-temporal characteristics of the received propagation paths are estimated by means of a super-resolution estimation algorithm. Lastly, for a road tunnel, many papers deal with channel characterization for predicting the performance of a Multiple-Input Multiple-Output (MIMO) link, without or with polarization diversity [6].

The objective of this contribution is to extend these previous experimental works for studying the time domain channel response for ultra wide band (UWB) applications. Frequency domain measurements have thus been carried out in a straight road tunnel, and in a band extending from 2.8 GHz to 5 GHz. Time domain analysis was then performed through Fourier Transform.

This paper is organized as follows: Section II briefly recalls the methodology of the measurement campaigns while Section III presents results on the mean path loss, small scale fading and delay spread. An analysis of the waveform of the received signal as a function of the distance between the transmitter and the receiver is detailed in Section IV and the correlation between signals received at different positions is also studied.

II. DESCRIPTION OF THE MEASUREMENT CAMPAIGN

Measurements took place in a straight arched tunnel, 3 km long. Its transverse section was semicircular and the diameter of the cylindrical part was 8.6 m. The maximum height was 6.1 m at the center of the tunnel. The tunnel was nearly free of obstacles like road signs, lamps, cables, etc. Furthermore the roughness of the walls was rather small, on the order of few cm. The tunnel was closed to traffic and consequently, the channel can be considered as stationary during the experiments. The transmitting (Tx) and receiving (Rx) antennas were wideband conical antennas, their gain being nearly flat in the bandwidth of interest.

Both Tx and Rx antennas were mounted on a rail, put at 1 m above ground and allowing their displacement, controlled by a step by step motor, on a maximum distance of 33 cm. During this measurement campaign, these rails were put perpendicular to the tunnel axis. The spatial step in this transverse plane was 3 cm, corresponding to half a wavelength at 5 GHz. This leads, for each axial distance D between Tx and Rx and for each frequency, to a set of 144 values of the channel transfer function H. The axial step was chosen to be equal to 4 m when 50 m < D < 202 m and to 6 m when 202 m < D < 500 m. Tx and Rx were not moving during measurements and thus the Doppler effect was avoided.

The channel sounder was based on a vector network analyzer (VNA). The Rx antenna was directly connected to one port of the VNA using a low attenuation coaxial cable and a 30 dB low-noise amplifier. To be able to make measurements up to 500 m, the signal of the Tx port of the VNA was converted into an optical signal, which was sent through fibre optics. The frequency step is 1.37 MHz from 2.8 to 5 GHz, leading to 1601 frequency points.

More details concerning the utilized system and experimental aspects of this study can be found in [7]. One can also mention that for this type of channel, the main contribution at large distance comes from multiple reflections of rays impinging the tunnel walls under a

 ISBN: 978-1-61208-123-6

grazing angle of incidence. Furthermore path loss strongly decreases for frequencies such that the transverse dimensions of the tunnel are much larger than the wavelength λ. However, when the roughness of the walls becomes on the order of λ, diffusion effect may counterbalance this decrease of path loss.

III. MEAN PATH LOSS, SMALL SCALE FADING AND DELAY SPREAD

In narrow band communication systems, path loss is frequency and distance dependent, while small scale fading is due to constructive and destructive interference of all possible paths between Tx and Rx. For UWB signals the most important characteristics are related to the variation of the energy of the pulse and not of its individual spectral components. Table 1 gives the value of the path loss defined as the value of the received power averaged over the whole frequency band, and normalized to the transmitted power.

TABLE I. MEAN PATH LOSS

Distance (m)	100	200	300	400	500
Path loss (dB)	82	83.1	84.2	85.5	86

We clearly see the guiding effect of the tunnel, the additional attenuation between 100 m and 500 m being only 4 dB.

To determine the characteristics of the small-scale fading, we consider a rectangular grid containing successive Rx positions. The width of the grid, i.e., its dimension along the transverse axis is equal to 33 cm and corresponds to the maximum displacement of the antenna in the transverse plane. Along the tunnel axis, we consider 3 successive distances as shown in Figure 1. Thus the length of the grid is either 8 m or 12 m depending if the distance *D* between Tx and Rx is smaller or larger than 200 m, as explained in Section I.

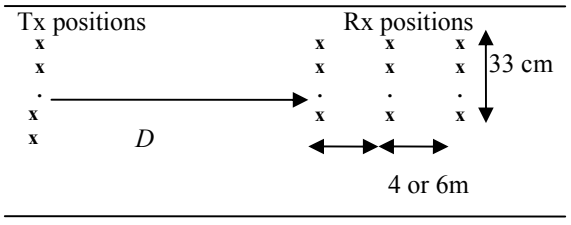

Figure 1. Successive positions of the Tx and Rx antennas. The transverse dimension of the tunnel is 8.6 m. The antennas are situated in the middle of one lane of this 2-lane tunnel.

The standard deviation ("*std*") of the path loss in the rectangular grid, normalized to its average value in this grid, was calculated for successive values of *D* varying between 50 m and 480 m and by also considering the 12 possible positions of the Tx antenna in the transverse plane of the tunnel. Curve in Figure 2 shows that *std* does not vary appreciably with the distance and remains on the order of 15%. This means that there is almost no fading as a result of interference and this is the same conclusion as in the case of propagation in typical in-building environment [8], [9], [10].

The time domain analysis of the propagation channel is based on measurement results in the frequency domain by applying a Fourier transform. For each axial distance *D*, the average delay spread is deduced from the channel impulse response (CIR) calculated for each of the 12x12, i.e., 144 channels associated to the possible positions of the antennas in the transverse plane. As shown in Table II, the delay spread remains nearly constant, whatever the distance.

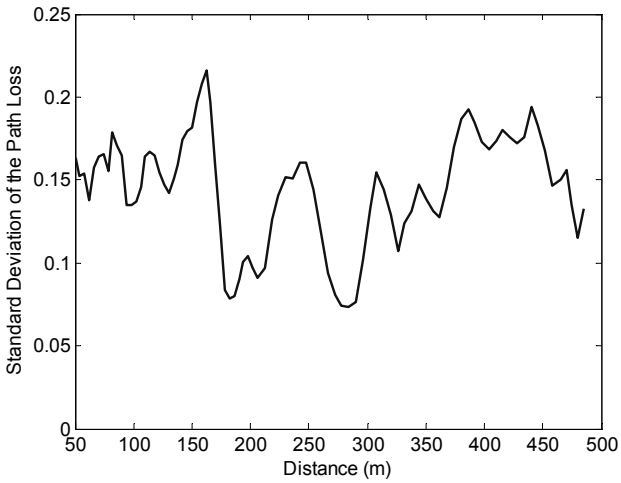

Figure 2. Standard deviation of the normalized path loss.

TABLE II. MEAN DELAY SPREAD

Distance (m)	100	200	300	400	500
Mean delay spread (ns)	2.5	1.7	2	1.8	2

This result is strongly related with the direction of the rays joining the transmitter and the receiver. In the horizontal plane, and for each value of *D*, the Angle of Arrival (AoA) and the angle of Departure (AoD) of the various rays can be deduced from measurements of the channel transfer function at various points in the transverse plane, by using high resolution estimation techniques, as the Space-alternating Generalized Expectation-maximization (SAGE) algorithm [11].

The variation of the angular spread A_s of the AoA and AoD is plotted in Figure 3. At 50 m from Tx, the angular spread is equal to about 12° and then continuously decreases with distance. The fact that the delay spread remains constant can thus be explained by this decrease of A_s with distance, which leads to rather constant time intervals between the successive rays. Consequently, the slope of the power delay profile becomes independent on the distance. It must be emphasized that measurements were done in static conditions and in an empty tunnel. In more realistic

 ISBN: 978-1-61208-123-6

situations, i.e., in presence of vehicles or obstacles, one can expect to get additional reflected signals but mainly if these obstacles are situated in the vicinity of the Rx antenna. This will lead to a slight increase of the delay spread but the previous conclusions may remain valid. One can mention that the results of narrowband and wideband propagation measurements conducted at 900 and 1800 MHz in five tunnels and described in [4] include the effects of pedestrians, vehicles, and curvature on propagation. A narrowband analysis showing the effects of vehicles is also presented in [12].

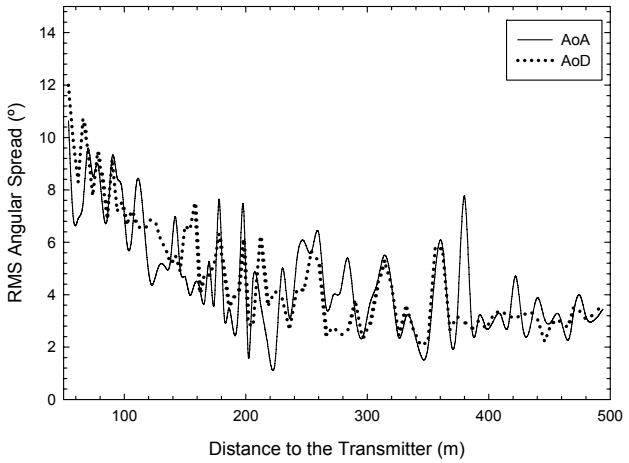

Figure 3. Angular spread of the direction of arrival and direction of departure of the rays.

IV. TIME DISPERSION AND CORRELATION

In this section, the change of the waveform of the pulse propagating in the tunnel is studied. Furthermore, the correlations between the transmitted pulse and the received pulse, on one hand, and between pulses received at different distances on the other hand, are emphasized.

A. Time dispersion

As previously outlined in Section II, the complex channel transfer function is measured in the frequency domain between 2.8 and 5 GHz. To get a real-value transmitted pulse, this transfer function is combined with its complex conjugate in the negative frequency domain before applying a Fourier transform. To avoid numerous oscillations, a Hamming window is used and the equivalent transmitted pulse is thus represented in Figure 4. Its peak amplitude is normalized to unity. The pseudo frequency corresponds to the center of the frequency band under analysis (3.9 GHz).

The pulses, which would be received at a distance of 50 m and 54 m start at 165 ns and 180 ns, respectively. However, to make an easiest comparison between these two pulses, they have been shifted in the time domain as in Figure 5 (a) and (b) to start at the same time. The origin of the time axis is quite arbitrary.

We observe a first cluster, which includes the direct path and a succession of other clusters corresponding to multipath propagation. Within this kind of clusters, the waveform may strongly vary with distance.

This means that at a distance D_1, the signal may be positive at a given time but may become negative at the same time at another distance D_2. By adding the signals measured at successive distances but shifted to start at the same time, one can thus expect to visualize the coherence between the signals received along the tunnel axis. This qualitative approach leads to curve (c) in Figure 5, this signal being obtained by averaging the waveforms at 50, 54 and 58 m. We observe, as expected, a decrease in amplitude of clusters associated with multipath propagation.

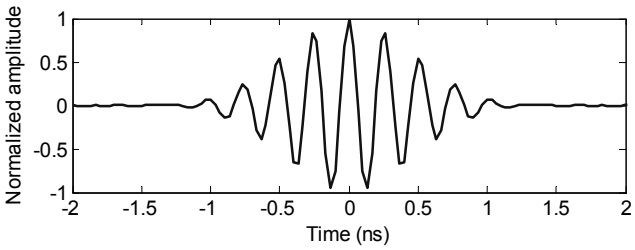

Figure 4. Equivalent transmitted pulse

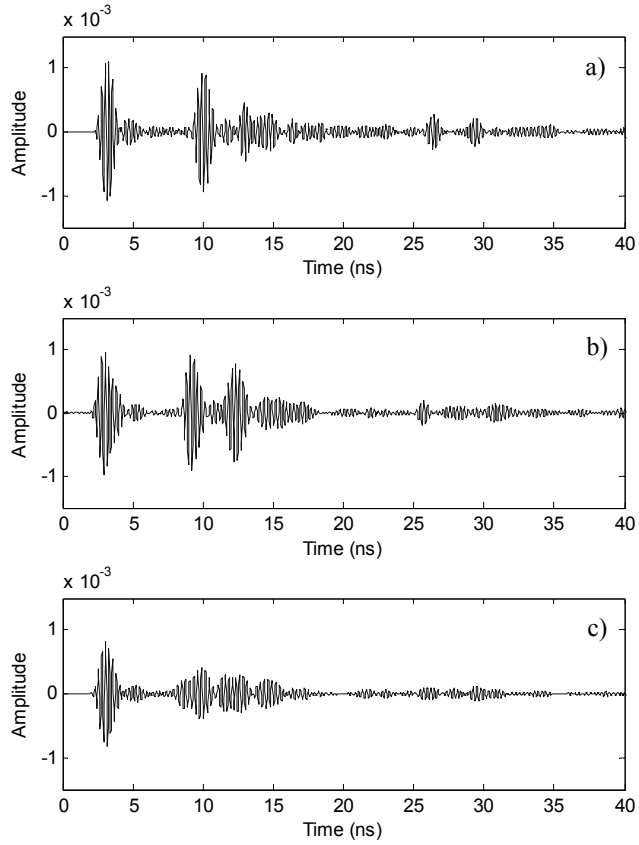

Figure 5. Waveforms of the pulse received at a distance of 50 m (curve (a), and at 54 m (curve (b). Curve (c) is the sum of the waveforms received at 50, 54 and 58 m and aligned in time domain. The origin of the time axis is thus quite arbitrary.

One can do the same approach to visualize the coherence in the transverse plane. Let us consider, for example, a distance of 50 m between Tx and Rx.

To plot the curve in Figure 6, the 144 signals obtained by combining the 12 possible positions of both Rx and Tx in the transverse plane, have been summed. We see that all clusters, except the one, which includes the direct path, have negligible amplitude.

The received power and the channel impulse response can be easily deduced from the amplitude of the received signal and from the correlation between the transmitted signal and the received signal.

A quantitative approach of the correlation is presented in the next paragraphs.

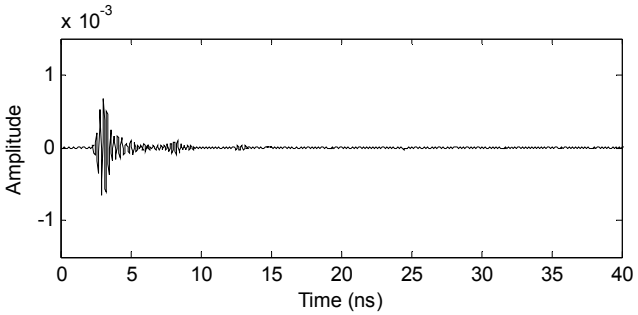

Figure 6. Average waveform by summing signals received in the transverse plane.

B. Transverse correlation

For a given axial distance D, one can compute the correlation, in the transverse plane, between the signal received by one Rx antenna and the signal received by the 11 others, the spatial step being 3 cm. This correlation is calculated for each of the 12 positions of the transmitter. This allows getting the average value of the correlation between the received signals in the transverse plane; the maximum distance between the receiving points being 33 cm. Results are presented in Figure 7 for three values of the axial distance D.

If we first consider a distance of 102 m, we see that the correlation coefficient rapidly decreases and reaches 0.5 for a distance between receiving points of 9 cm. For larger axial distance D, 314 and 498 m in this example, the slope of the decrease is less important.

This result can be explained in frequency domain by the modal approach of the propagation of electromagnetic waves in the tunnel, which acts as an oversize waveguide. At large distances, the number of modes significantly contributing to the received power decreases. This gives rise to a more coherent transverse field [7].

C. Axial correlation

Due to experimental constraints, the successive points of measurements along the tunnel axis were 4 m or 6 m apart, depending on the distance D. This distance is not small enough to clearly point out the decrease of the correlation ρ_{ax} between signals. Indeed, for the first step, i.e., at 4 m, the correlation coefficient between Rx points situated at $D = 50$ m and at $D = 54$ m is already equal to 0.4.

The only point, which could be studied is the variation of ρ_{ax} between points situated at $D = z$ and at $D = z + 4$ or at $D = z + 6$, when z varies from 50 m up to 500 m.

The calculation shows that ρ_{ax} increases from 0.4 for $z = 50$ m to 0.7 for $z = 500$ m. This can be explained, as in the case of the correlation in the transverse plane, by the decrease of the number of propagating modes at large distance from the transmitter.

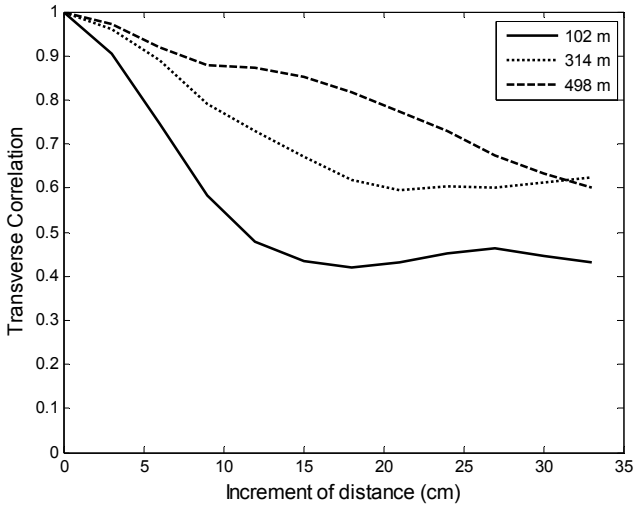

Figure 7. Correlation in the transverse plane

V. CONCLUSION

In this contribution, the time domain channel characteristics for a tunnel environment have been studied. The guiding effect of the tunnel clearly appears on the mean path loss, the small scale fading related to the energy of the UWB pulse being very small as it is the case for in-building environment.

The signals received at different locations in the transverse plane of the tunnel are rapidly uncorrelated, the correlation coefficient being equal to 0.5 if the receiving points are 9 cm apart.

However the correlation increases at large distance of the transmitter due to the attenuation of high order propagating modes, which leads to a decrease of the number of modes playing a non negligible role in the received signal.

Further work will be to develop a time domain statistical model, based on measurement results. This model will then be used to extend the physical layer approach described in this paper to simulate a communication link, taking the modulation scheme into account, in order to predict flow throughput and bit error rate.

ACKNOWLEDGMENT

This work has been supported by the Fundación Séneca de la Región de Murcia (14809/EFPI/10 and 06640/FPI/07) in the frame of PCTRM 2007-2010 with foundation of INFO

and FEDER funds of up to 80%; Ministerio de Industria, Turismo y Comercio (Spain), under the project CORAGE (TSI-0201100-2009-653); and by the European FEDER funds, the Region Nord Pas de Calais and the French Ministry of Research, as part of the CISIT project (France).

REFERENCES

[1] A. Chehri and P. Fortier, "Frequency Domain Analysis of UWB Channel Propagation in Underground Mines", Proc. IEEE Conf. on Vehicular Techno., 25-28 Sept. 2006, 5p.,

[2] A. Chehri, P. Fortier, and P. M. Tardif, "Characterization of the Ultra-Wideband Channel in Confined Environments with Diffracting Rough Surfaces', Wireless Personal Communications, Aug. 2010, pp. 1-19, DOI: 10.1007/s11277-010-0097-2,

[3] M. Lienard and P. Degauque, "Propagation in Wide Tunnels at 2 GHz: A Statistical Analysis", IEEE Trans. on Vehicular Techno., vol. 47, no. 4, Nov. 1998, pp. 1322 – 1328,.

[4] Y. P. Zhang and Y. Hwang, "Characterization of UHF Radio Propagation Channels in Tunnel Environments for Microcellular and Personal Communications", IEEE Trans on Vehicul. Techno., vol. 47, no. 1, Feb. 1998, pp. 283 – 296.

[5] G. S. Ching, G.S., M. Ghoraishi, M .Landmann, M., N. Lertsirisopon, J. Takada, T. Imai, I. Sameda, and H. Sakamoto, " Wideband Polarimetric Directional Propagation Channel Analysis Inside an Arched Tunnel", IEEE Trans. on Antennas and Propag., vol. 57, March 2009, pp. 760-767.

[6] J.-M. Molina-Garcia-Pardo, M. Lienard, P. Degauque, C. García-Pardo, and L. Juan-Llacer, "MIMO channel capacity with polarization diversity in arched tunnels", IEEE Antennas and Wireless Propagation Letters, vol. 8, 2009, pp. 1186-1189.

[7] J.-M. Molina-Garcia-Pardo, M. Lienard, and P. Degauque, "Propagation in Tunnels: Experimental Investigations and Channel Modeling in a Wide Frequency Band for MIMO Applications" EURASIP J. on Wireless Com. and Networking,, 2009, Article ID 560571, 9 pages, doi:10.1155/2009/560571.

[8] A. Muqaibel, A. Safaai-Jazi, A. Attiya, B. Woerner, and S. Riad, "Path loss and time dispersion parameters for indoor UWB propagation", IEEE Trans. on Wireless Comm., vol. 5, March 2006, pp. 550-559.

[9] A. F. Molisch, "Ultra-wide band propagation channels", Proc. of the IEEE, vol. 97, Feb. 2009, pp. 353-371.

[10] M. Z. Win and R. A. Scholtz, "Characterization of ultra-wideband wireless indoor channels: a communication-theoric view", IEEE J. on Selected Areas in Com., vol. 20, Dec. 2002, pp. 1613-1627.

[11] J. A. Fessler and A. O. Hero, "Space-alternating generalized expectation-maximization algorithm," *IEEE Trans. on Signal Processing*, vol. 42, no.10, Oct. 1994, pp. 2664–2677, Oct 1994.

[12] M. Liénard, S. Bétrencourt, and P. Degauque, "Propagation in Road Tunnels: a Statistical Analysis of the Field Distribution and Impact of the Traffic", Annales des Télécom., vol 55, n° 11-12, Dec. 2000, pp. 623-631.

 ISBN: 978-1-61208-123-6